symmetry

MDPI

Article

A Novel Probabilistic Approach Based on Trigonometric Function: Model, Theory with Practical Applications

Omalsad Hamood Odhah [1], Huda M. Alshanbari [1], Zubair Ahmad [2,*], Faridoon Khan [3] and Abd Al-Aziz Hosni El-Bagoury [4]

1 Department of Mathematical Sciences, College of Science, Princess Nourah bint Abdulrahman University, P.O. Box 84428, Riyadh 11671, Saudi Arabia; ohodhah@pnu.edu.sa (O.H.O.); hmalshanbari@pnu.edu.sa (H.M.A.)
2 Department of Statistics, Quaid-i-Azam University, Islamabad 44000, Pakistan
3 Pakistan Institute of Development Economics, Islamabad 44000, Pakistan; faridoon.marwat@gmail.com
4 Basic Sciences Department, Higher Institute of Engineering and Technology, EL-Mahala EL-Kobra 31511, Egypt; azizhel2013@yahoo.com
* Correspondence: z.ferry21@gmail.com; Tel.: +92-345-9375162

Abstract: Proposing new families of probability models for data modeling in applied sectors is a prominent research topic. This paper also proposes a new method based on the trigonometric function to derive the updated form of the existing probability models. The proposed family is called the cotangent trigonometric-*G* family of distributions. Based on the cotangent trigonometric-*G* method, a new version of the Weibull model, namely, the cotangent trigonometric Weibull distribution, is studied. Certain mathematical properties of the cotangent trigonometric-*G* family are derived. The estimators of the cotangent trigonometric-*G* distributions are obtained via the maximum likelihood method. The Monte Carlo simulation study is conducted to assess the performances of the estimators. Finally, two applications from the health sector are considered to illustrate the cotangent trigonometric-*G* method. Based on seven evaluating criteria, it is observed that the cotangent trigonometric-*G* significantly improves the fitting power of the existing models.

Keywords: cotangent function; trigonometric function; Weibull distribution; distributional properties; medical datasets; statistical modeling

Citation: Odhah, O.H.; Alshanbari, H.M.; Ahmad, Z.; Khan, F.; El-Bagoury, A.A.-A.H. A Novel Probabilistic Approach Based on Trigonometric Function: Model, Theory with Practical Applications. *Symmetry* **2023**, *15*, 1528. https://doi.org/10.3390/sym15081528

Academic Editor: Qing-Wen Wang

Received: 19 June 2023
Revised: 13 July 2023
Accepted: 21 July 2023
Published: 2 August 2023

1. Introduction

It is a well-established and proven fact that no particular probability distribution can provide an adequate fit in all situations. Therefore, almost every sector of life needs to generate new probability distributions with updated distributional flexibility and new criteria. This fact has diverted the attention of researchers and encouraged them to explore new potential statistical distributions with practical implications in different areas of life. In the literature, a considerable number of papers have been published that have introduced new probability distributions to adequately fit data in various fields of applied sciences [1–14].

Among the probability distributions developed and implemented in the literature, the Weibull model occupies an important place [15,16]. Due to the simplest form of the probability density function (PDF), nice physical interpretation of the parameters, and a closed form of the cumulative distribution function (CDF), the Weibull distribution has attracted researchers to keep it on top of the list for analyzing real-world phenomena (i.e., practical applications or real-life datasets); see [17].

Let $G(w;\boldsymbol{\xi})$ be the CDF and $g(w;\boldsymbol{\xi})$ be the PDF of the Weibull distribution with $\sigma \in \mathbb{R}^+$ (scale parameter) and $\alpha \in \mathbb{R}^+$ (shape parameter). The CDF of the Weibull distributed random variable $W \in \mathbb{R}^+$, is given by

$$G(w;\boldsymbol{\xi}) = 1 - e^{-\sigma w^{\alpha}}, \qquad w \in \mathbb{R}^+, \tag{1}$$

with PDF $g(w;\boldsymbol{\xi})$ given by

$$g(w;\boldsymbol{\xi}) = \alpha\sigma w^{\alpha-1}e^{-\sigma w^{\alpha}}, \qquad w \in \mathbb{R}^{+}, \tag{2}$$

where $\boldsymbol{\xi} = (\alpha, \sigma)$.

To be fair, the Weibull distribution has always been the first choice of researchers to apply for modeling data that have a single-state failure rate. Of course, it provides an excellent fit for such a of dataset in almost every field of life. Unfortunately, however, the Weibull distribution does not provide a good fit for datasets that do not have failure rates in a single state [18–21]. To address this shortcoming of the Weibull distribution, a series of modified versions of the Weibull distribution have been considered and implemented. For detailed reviews of such modifications to the Weibull distribution, we refer to [22,23].

Thanks to these modified versions of the Weibull distribution, many of them have achieved the desired goals to provide the best fit to the mixed-state failure rate data. But, on the other hand, the number of model parameters also increased rapidly. In fact, some of these modified versions have parameters increased to six or even seven parameters [24].

It is an obvious fact that sometimes introducing a new probability distribution with additional parameter(s) can lead to a re-parameterization and estimation problem. Therefore, to avoid the re-parameterization problems that arise from adding new parameters, we introduce a new trigonometric-based family of distributions. The new family is introduced by incorporating the cotangent function and can be called the new cotangent-*G* (NCT-*G*) family of distributions. An interesting fact about the NCT-*G* family is that it has no additional parameters.

Definition 1. *Suppose $W \in \mathbb{R}$ has the family of NCT-G distributions without any additional parameters. Then, its CDF $F(w;\boldsymbol{\xi})$ is given by*

$$F(w;\boldsymbol{\xi}) = 1 - \frac{\bar{G}(w;\boldsymbol{\xi})}{e^{\cot\left[\frac{\pi}{2}\bar{G}(w;\boldsymbol{\xi})\right]}}, \qquad w \in \mathbb{R}, \tag{3}$$

with PDF $f(w;\boldsymbol{\xi}) = \frac{d}{dw}F(w;\boldsymbol{\xi})$, given by

$$f(w;\boldsymbol{\xi}) = \frac{g(w;\boldsymbol{\xi})}{e^{\cot\left[\frac{\pi}{2}\bar{G}(w;\boldsymbol{\xi})\right]}}\left[1 + \frac{\pi}{2}\bar{G}(w;\boldsymbol{\xi})\csc^{2}\left(\frac{\pi}{2}\bar{G}(w;\boldsymbol{\xi})\right)\right], \qquad w \in \mathbb{R}. \tag{4}$$

The survival function (SF) $S(w;\boldsymbol{\xi}) = 1 - F(w;\boldsymbol{\xi})$ of the NCT-G family is expressed by

$$S(w;\boldsymbol{\xi}) = \frac{\bar{G}(w;\boldsymbol{\xi})}{e^{\cot\left[\frac{\pi}{2}\bar{G}(w;\boldsymbol{\xi})\right]}}, \qquad w \in \mathbb{R}.$$

The hazard function (HF) $h(w;\boldsymbol{\xi}) = \frac{f(w;\boldsymbol{\xi})}{S(w;\boldsymbol{\xi})}$ of the NCT-G family is given by

$$f(w;\boldsymbol{\xi}) = \frac{g(w;\boldsymbol{\xi})}{\bar{G}(w;\boldsymbol{\xi})}\left[1 + \frac{\pi}{2}\bar{G}(w;\boldsymbol{\xi})\csc^{2}\left(\frac{\pi}{2}\bar{G}(w;\boldsymbol{\xi})\right)\right], \qquad w \in \mathbb{R}.$$

The cumulative HF (CHF) $H(w;\boldsymbol{\xi}) = -\log[S(w;\boldsymbol{\xi})]$ of the NCT-G family is

$$H(w;\boldsymbol{\xi}) = -\log\left(\frac{\bar{G}(w;\boldsymbol{\xi})}{e^{\cot\left[\frac{\pi}{2}\bar{G}(w;\boldsymbol{\xi})\right]}}\right), \qquad w \in \mathbb{R}.$$

In Section 2, we combine Equation (1) with the proposed cotangent-based method expressed by Equation (3) to obtain the CDF of the special member of the NCT-*G* family. The special member of the NCT-*G* family is a new variant of the Weibull distribution and can be called a new cotangent–Weibull (NCT-Weibull) distribution.

2. The NCT-Weibull Distribution

In this section, we present some important distributional functions of the NCT-Weibull model such as CDF, PDF, SF, HF, and CHF. In addition to mathematical descriptions, visual illustrations of these functions are also presented.

Assume $W \in \mathbb{R}^+$ follows the NCT-Weibull distribution with parameters $\alpha > 0$ and $\sigma > 0$. Its CDF $F(w;\boldsymbol{\xi})$ is given by

$$F(w;\boldsymbol{\xi}) = 1 - \frac{e^{-\sigma w^{\alpha}}}{e^{\cot\left(\frac{\pi}{2}e^{-\sigma w^{\alpha}}\right)}}, \qquad w \geq 0, \tag{5}$$

with PDF

$$f(w;\boldsymbol{\xi}) = \frac{\alpha\sigma w^{\alpha-1}e^{-\sigma w^{\alpha}}}{e^{\cot\left[\frac{\pi}{2}\bar{G}(w;\boldsymbol{\xi})\right]}}\left[1 + \frac{\pi}{2}e^{-\sigma w^{\alpha}}\csc^2\left(\frac{\pi}{2}e^{-\sigma w^{\alpha}}\right)\right], \qquad w > 0. \tag{6}$$

The SF $S(w;\boldsymbol{\xi})$ of the NCT-Weibull distribution is

$$S(w;\boldsymbol{\xi}) = \frac{e^{-\sigma w^{\alpha}}}{e^{\cot\left(\frac{\pi}{2}e^{-\sigma w^{\alpha}}\right)}}, \qquad w > 0.$$

The HF $h(w;\boldsymbol{\xi})$ of the NCT-Weibull distribution is

$$h(w;\boldsymbol{\xi}) = \frac{\alpha\sigma w^{\alpha-1}e^{-\sigma w^{\alpha}}}{e^{-\sigma w^{\alpha}}}\left[1 + \frac{\pi}{2}e^{-\sigma w^{\alpha}}\csc^2\left(\frac{\pi}{2}e^{-\sigma w^{\alpha}}\right)\right], \qquad w > 0.$$

The CHF $H(w;\boldsymbol{\xi})$ of the NCT-Weibull distribution is

$$H(w;\boldsymbol{\xi}) = -\log\left(\frac{e^{-\sigma w^{\alpha}}}{e^{\cot\left(\frac{\pi}{2}e^{-\sigma w^{\alpha}}\right)}}\right), \qquad w > 0.$$

The visual illustrations of $F(w;\boldsymbol{\xi})$ and $S(w;\boldsymbol{\xi})$ of the NCT-Weibull distribution are provided in Figure 1. The graphs of $F(w;\boldsymbol{\xi})$ and $S(w;\boldsymbol{\xi})$ are obtained for different values of α and σ using the range of W between 0 and 3; see w-axis of Figure 1. The plots in Figure 1 confirm that the NCT-Weibull distribution has a valid CDF, as the curves of $F(w;\boldsymbol{\xi})$ lie between 0 and 1.

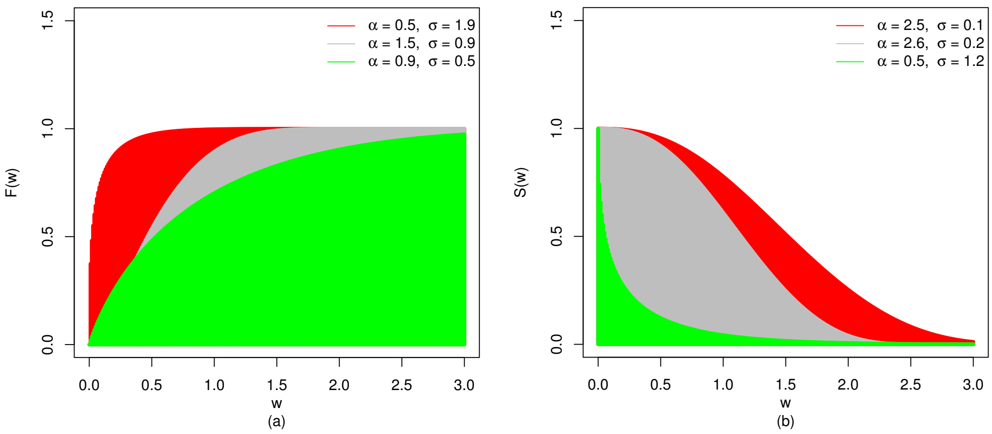

Figure 1. For different values of α and σ, the visual illustrations of (**a**) $F(w;\boldsymbol{\xi})$ and (**b**) $S(w;\boldsymbol{\xi})$ of the NCT-Weibull distribution.

The plots of $f(w;\boldsymbol{\xi})$ of the NCT-Weibull distribution are obtained for different values of α and σ using the range of W between 0 and 3; see w-axis of Figure 2. These plots show that $f(w;\boldsymbol{\xi})$ of the NCT-Weibull distribution has four different shapes, that is, (i) unimodal (red curve), (ii) right-skewed (grey curve), (iii) symmetrical (green curve), and (iv) left-skewed (black, magenta, and blue curves).

Furthermore, the plots of $h(w;\boldsymbol{\xi})$ of the NCT-Weibull distribution are also obtained for different values of α and σ using the range of W between 0 and 3; see w-axis of Figure 3. The plots in Figure 3 show that the NCT-Weibull distribution is able to capture two monotonic and two non-monotonic shapes of $h(w;\boldsymbol{\xi})$. The monotonic category includes increasing (red curve) and decreasing (grey curve) shapes of $h(w;\boldsymbol{\xi})$, whereas the non-monotonic category includes the bathtub (green curve) and modified unimodal (blue curve) shapes of $h(w;\boldsymbol{\xi})$. The modified unimodal failure rate function is also called an increasing–decreasing–increasing failure rate function.

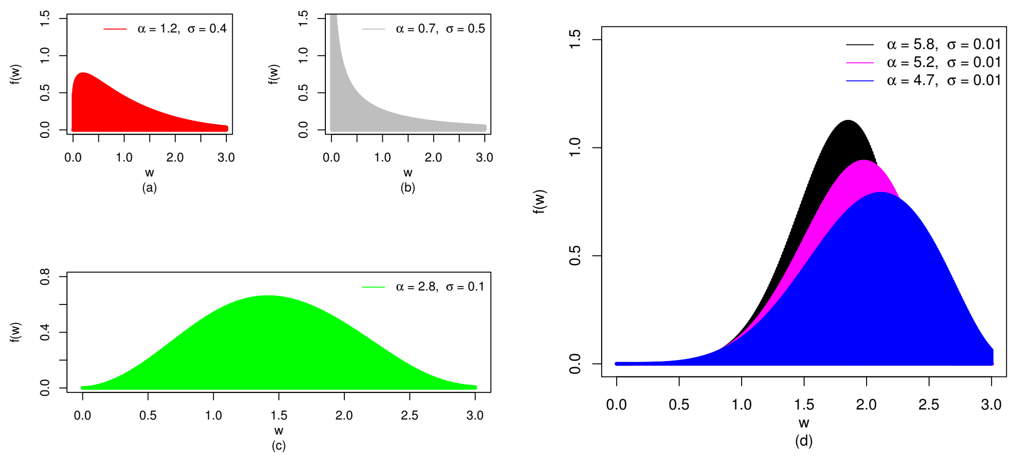

Figure 2. Different plots of $f(w;\boldsymbol{\xi})$ of the NCT-Weibull distribution, including (**a**) right-skewed, (**b**) decreasing, (**c**) symmetrical, and (**d**) left-skewed.

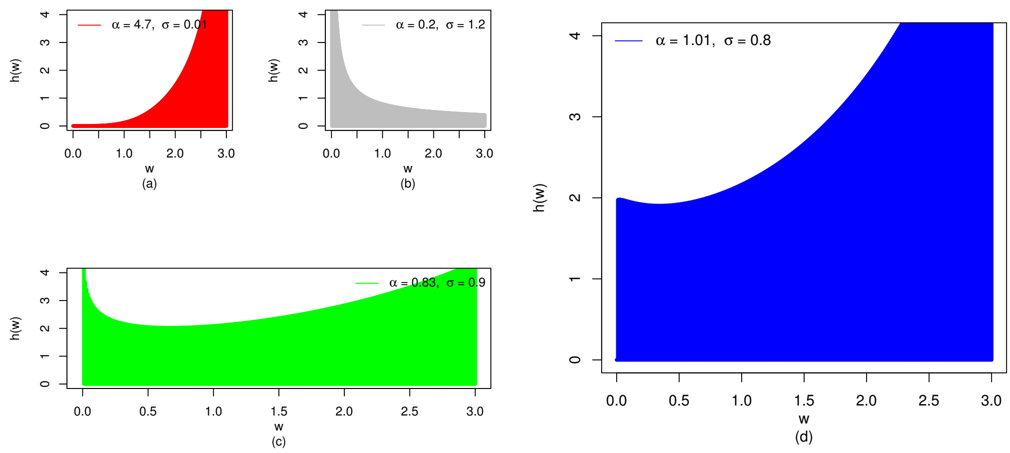

Figure 3. Different plots of $h(w;\boldsymbol{\xi})$ of the NCT-Weibull distribution, including (**a**) increasing, (**b**) decreasing, (**c**) bathtub, and (**d**) modified unimodal.

3. Distributional Properties

This section explores some mathematical properties of the NCT-G family of distributions such as the quantile function (QF), r^{th} moment, skewness, kurtosis, quartiles, and moment generating function (MGF). We only provide a manual derivation of these features. Statistical software (programming software), for example, Mathematica, Python, or R, can be implemented for numerical analysis of these properties/quantities.

3.1. The Quantile Function

This subsection explores the QF of the NCT-G distributions. Suppose $W \in \mathbb{R}$ follows the NCT-G distributions with CDF $F(w;\boldsymbol{\xi})$ and PDF $f(w;\boldsymbol{\xi})$. Then, its QF, denoted by w_q, is obtained by solving the inverse form of $F(w;\boldsymbol{\xi})$, as given by

$$w_q = F^{-1}(u), \tag{7}$$

where $0 < q < 1$, and u is the solution of

$$\cot(u) + \log(1 - q) - \log[1 - u] = 0.$$

3.2. The Quartile Measures, Skewness, and Kurtosis

In this subsection, we provide the quartile measures, skewness, and kurtosis of the NCT-*G* distributions.

- The first quartile of the NCT-*G* distributions, represented by Q_1 or $w_{\frac{1}{4}}$, is obtained as

$$w_{\frac{1}{4}} = F^{-1}(u),$$

where u is the solution of

$$\cot(u) + \log\left(1 - \frac{1}{4}\right) - \log[1 - u] = 0.$$

- The second quartile of the NCT-*G* distributions, represented by Q_2 or $w_{\frac{1}{2}}$, is obtained as

$$w_{\frac{1}{2}} = F^{-1}(u),$$

where u is the solution of

$$\cot(u) + \log\left(1 - \frac{1}{2}\right) - \log[1 - u] = 0.$$

- The third quartile of the NCT-*G* distributions, represented by Q_3 or $w_{\frac{3}{4}}$, is obtained as

$$w_{\frac{3}{4}} = F^{-1}(u),$$

where u is the solution of

$$\cot(u) + \log\left(1 - \frac{3}{4}\right) - \log[1 - u] = 0.$$

- The skewness of the NCT-*G* distributions (Galton's skewness) is derived as

$$\frac{Q_{2/8} - 2Q_{4/8} + Q_{6/8}}{Q_{6/8} - Q_{2/8}},$$

where the statistical quantities $Q_{2/8}, Q_{4/8}$, and $Q_{6/8}$ are obtained, respectively, by incorporating $q = \frac{2}{8}$, $q = \frac{4}{8}$, and $q = \frac{6}{8}$ in Equation (7).
- The kurtosis of the NCT-*G* distributions (Moor's kurtosis) is derived as

$$\frac{Q_{7/8} - Q_{5/8} - Q_{1/8} + Q_{3/8}}{Q_{6/8} - Q_{2/8}},$$

where the statistical quantities $Q_{1/8}, Q_{3/8}, Q_{5/8}$, and $Q_{7/8}$ are obtained, respectively, by incorporating $q = \frac{1}{8}$, $q = \frac{3}{8}$, $q = \frac{5}{8}$, and $q = \frac{7}{8}$ in Equation (7).

Table 1 presents a comprehensive overview of the quantile values, as well as the corresponding coefficients of skewness (β_1) and kurtosis (β_2), obtained for various q values and parameter configurations. This table serves as a valuable resource for examining the statistical properties and asymmetry characteristics of the proposed model. The coefficients of skewness (β_1) provided in the table serve as indicators of the symmetry or asymmetry of the proposed model's distribution. Positive values of β_1 indicate a right-skewed distribution, suggesting a longer right tail and a concentration of observations towards the left. Conversely, negative values of β_1 signify a left-skewed distribution, characterized by a longer left tail and a concentration of observations towards the right. Furthermore, a graphical representation of the skewness and kurtosis of the proposed distribution is also presented in Figure 4.

Table 1. Numerical values for quartiles along with coefficients of skewnenss and kurtosis of the NCT-Weibull distribution.

Parameters		Measures				
σ	α	Q_1	Q_2	Q_3	β_1	β_2
0.25	0.25	0.0450	1.6655	27.2954	0.8811	4.4220
	0.7	0.3304	1.1998	3.2575	0.4059	1.4424
	1.0	0.4606	1.1360	2.2857	0.2599	1.2547
	1.5	0.5964	1.0887	1.7353	0.1354	1.1798
	2.5	0.7334	1.0522	1.3918	0.0316	1.1715
	4.0	0.8239	1.0324	1.2296	−0.0278	1.1887
0.7	0.25	0.0007	0.0272	0.4441	0.8806	4.4202
	0.7	0.0759	0.2756	0.7484	0.4060	1.4422
	1.0	0.1645	0.4057	0.8163	0.2598	1.2552
	1.5	0.3002	0.5480	0.8733	0.1352	1.1803
	2.5	0.4858	0.6972	0.9221	0.0307	1.1718
	4.0	0.6368	0.7981	0.9505	−0.0282	1.1883
1.0	0.25	0.0001	0.0065	0.1066	0.8810	4.42203
	0.7	0.0457	0.1654	0.4496	0.4071	1.4428
	1.0	0.1152	0.2840	0.5715	0.2600	1.2545
	1.5	0.2367	0.4321	0.6886	0.1353	1.1802
	2.5	0.4212	0.6045	0.7994	0.0309	1.1711
	4.0	0.5825	0.7300	0.8695	−0.0280	1.1888
1.5	0.25	0.5825	0.7300	0.8695	−0.0280	1.1888
	0.7	0.0254	0.0928	0.2519	0.4046	1.4421
	1.0	0.0767	0.1894	0.3808	0.2592	1.2551
	1.5	0.1807	0.3297	0.5255	0.1355	1.1800
	2.5	0.3581	0.5140	0.6799	0.0313	1.1705
	4.0	0.5263	0.6596	0.7856	−0.0284	1.1890
2.5	0.25	4×10^{-6}	0.0005	0.0028	0.6667	4.4566
	0.7	0.0123	0.0447	0.1214	0.4059	1.4439
	1.0	0.0460	0.1136	0.2285	0.2590	1.2562
	1.5	0.1285	0.2346	0.3738	0.1353	1.1803
	2.5	0.2921	0.4189	0.5541	0.0318	1.1721
	4.0	0.4634	0.5806	0.6914	−0.0278	1.1899
4.0	0.25	6×10^{-7}	0.0005	0.0007	−0.3333	2.1218
	0.7	0.0064	0.0230	0.0620	0.4017	1.4498
	1.0	0.0290	0.0711	0.1430	0.2603	1.2565
	1.5	0.0939	0.1713	0.2734	0.1377	1.1792
	2.5	0.2419	0.3470	0.4592	0.0324	1.1705
	4.0	0.4119	0.5162	0.6149	−0.0277	1.1879

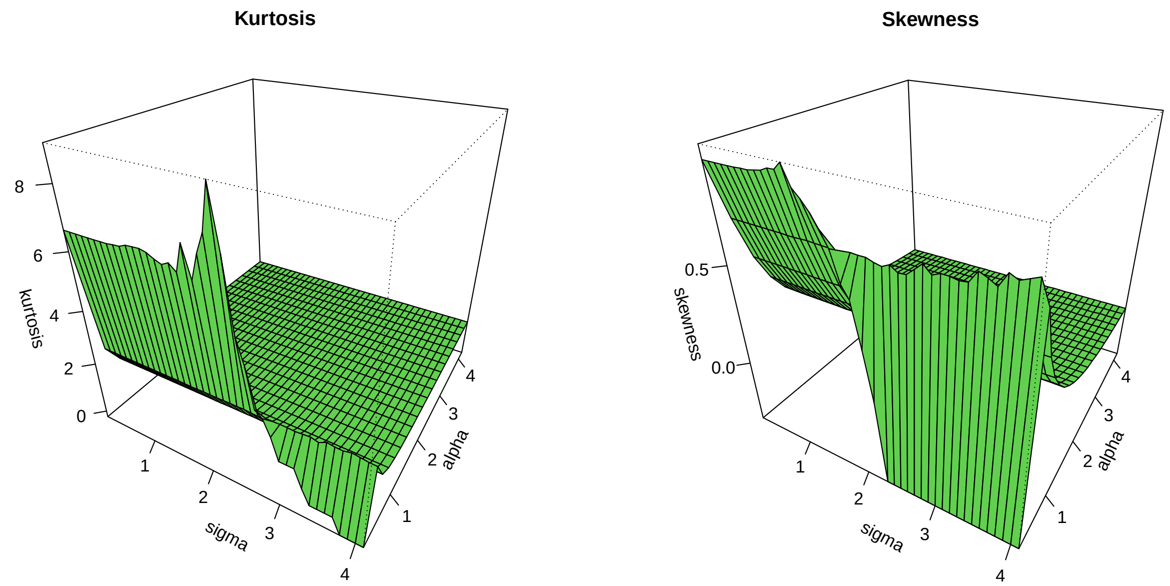

Figure 4. A graphical illustration of the coefficients of skewness and kurtosis of the NCT-Weibull distribution.

3.3. The r^{th} Moment and MGF of the NCT-G Distributions

This subsection offers the mathematical derivation of the r^{th} moment (denoted by μ_r') and MGF (denoted by $M_t(w)$) of the NCT-G distributions. Suppose $W \in \mathbb{R}$ has the NCT-G distributions with PDF $f(w;\boldsymbol{\xi})$; its r^{th} moment is derived as

$$\mu_r' = \int_{\Omega} w^r f(w;\boldsymbol{\xi}) dw. \tag{8}$$

Using Equation (4) in (8), we have

$$\mu_r' = \int_{\Omega} w^r \frac{g(w;\boldsymbol{\xi})}{e^{\cot\left[\frac{\pi}{2}\bar{G}(w;\boldsymbol{\xi})\right]}} \left[1 + \frac{\pi}{2}\bar{G}(w;\boldsymbol{\xi}) \csc^2\left(\frac{\pi}{2}\bar{G}(w;\boldsymbol{\xi})\right)\right] dw. \tag{9}$$

Using the series

$$e^w = \sum_{i=1}^{\infty} \frac{w^i}{i!}. \tag{10}$$

Using $w = \cot\left[\frac{\pi}{2}\bar{G}(w;\boldsymbol{\xi})\right]$ in Equation (10), we obtain

$$e^{\cot\left[\frac{\pi}{2}\bar{G}(w;\boldsymbol{\xi})\right]} = \sum_{i=1}^{\infty} \frac{\left(\cot\left[\frac{\pi}{2}\bar{G}(w;\boldsymbol{\xi})\right]\right)^i}{i!}. \tag{11}$$

Incorporating Equation (11) in (9), we have

$$\mu_r' = \sum_{i=1}^{\infty} \frac{1}{i!} \int_{\Omega} w^r g(w;\boldsymbol{\xi}) \left(\cot\left[\frac{\pi}{2}\bar{G}(w;\boldsymbol{\xi})\right]\right)^i \left[1 + \frac{\pi}{2}\bar{G}(w;\boldsymbol{\xi}) \csc^2\left(\frac{\pi}{2}\bar{G}(w;\boldsymbol{\xi})\right)\right] dw,$$

$$\mu_r' = \sum_{i=1}^{\infty} \frac{1}{i!} \int_{\Omega} w^r g(w;\boldsymbol{\xi}) \left(\cot\left[\frac{\pi}{2}\bar{G}(w;\boldsymbol{\xi})\right]\right)^i dw$$
$$+ \frac{\pi}{2} \sum_{i=1}^{\infty} \frac{1}{i!} \int_{\Omega} w^r g(w;\boldsymbol{\xi}) \bar{G}(w;\boldsymbol{\xi}) \left(\cot\left[\frac{\pi}{2}\bar{G}(w;\boldsymbol{\xi})\right]\right)^i \csc^2\left(\frac{\pi}{2}\bar{G}(w;\boldsymbol{\xi})\right) dw,$$

$$\mu_r' = \sum_{i=1}^{\infty} \frac{1}{i!} [\Delta_{1,i}(t;\boldsymbol{\eta}) + \Delta_{2,i}(t;\boldsymbol{\eta})],$$

where

$$\Delta_{1,i}(t;\boldsymbol{\eta}) = \int_{\Omega} w^r g(w;\boldsymbol{\xi}) \left(\cot\left[\frac{\pi}{2}\bar{G}(w;\boldsymbol{\xi})\right]\right)^i dw,$$

and

$$\Delta_{2,i}(t;\boldsymbol{\eta}) = \int_{\Omega} w^r g(w;\boldsymbol{\xi})\bar{G}(w;\boldsymbol{\xi}) \left(\cot\left[\frac{\pi}{2}\bar{G}(w;\boldsymbol{\xi})\right]\right)^i \csc^2\left(\frac{\pi}{2}\bar{G}(w;\boldsymbol{\xi})\right) dw.$$

The MGF $M_t(w)$ of the NCT-G distributions is obtained as

$$M_t(w) = E\left(e^{tw}\right) = \sum_{r=1}^{\infty} \frac{t^r}{r!} \int_{\Omega} w^r f(w;\boldsymbol{\xi}) dt.$$

Finally, we obtain

$$M_t(w) = \sum_{r=1}^{\infty}\sum_{i=1}^{\infty} \frac{t^r}{i!r!}[\Delta_{1,i}(t;\boldsymbol{\eta}) + \Delta_{2,i}(t;\boldsymbol{\eta})].$$

4. Estimation and Simulation

This section presents the estimation of the parameters (α, σ) of the NCT-Weibull distribution. The estimation process is carried out using the maximum likelihood method. In addition to the mathematical derivation of the maximum likelihood estimators (MLEs) $(\hat{\alpha}_{MLE}, \hat{\sigma}_{MLE})$ of the parameters of the NCT-Weibull distribution, a simulation study (SS) is also performed. The SS is performed to test how $\hat{\alpha}_{MLE}$ and $\hat{\sigma}_{MLE}$ show performance.

4.1. Estimation

Assume a set of samples, say $W_1, W_2, ..., W_n$, with values $w_1, w_2, ..., w_n$, observed randomly from the NCT-Weibull distribution with PDF $f(w;\boldsymbol{\xi})$. Then, corresponding to $f(w;\boldsymbol{\xi})$, the likelihood function (LF), expressed by $\delta(\alpha, \sigma)$, is given by

$$\delta(\alpha, \sigma) = \prod_{i=1}^{n} f(w_i;\boldsymbol{\xi}). \tag{12}$$

Using Equation (6) in (12), we obtain

$$\delta(\alpha, \sigma) = \prod_{i=1}^{n} \frac{\alpha\sigma w_i^{\alpha-1} e^{-\sigma w_i^{\alpha}}}{e^{\cot\left[\frac{\pi}{2}e^{-\sigma w_i^{\alpha}}\right]}} \left[1 + \frac{\pi}{2}e^{-\sigma w_i^{\alpha}} \csc^2\left(\frac{\pi}{2}e^{-\sigma w_i^{\alpha}}\right)\right]. \tag{13}$$

Corresponding to $\delta(\alpha, \sigma)$ presented in Equation (13), the log-likelihood function (LLF), say $\lambda(\alpha, \sigma)$, is given by

$$\lambda(\alpha, \sigma) = n\log\alpha + n\log\sigma + (\alpha - 1)\sum_{i=1}^{n}\log w_i - \sigma\sum_{i=1}^{n} w_i^{\alpha} - \sum_{i=1}^{n}\cot\left[\frac{\pi}{2}e^{-\sigma w_i^{\alpha}}\right]$$
$$+ \sum_{i=1}^{n}\log\left[1 + \frac{\pi}{2}e^{-\sigma w_i^{\alpha}} \csc^2\left(\frac{\pi}{2}e^{-\sigma w_i^{\alpha}}\right)\right]. \tag{14}$$

The maximum likelihood estimators (MLEs) can be obtained by maximizing Equation (4) with respect to the unknown parameters. However, it is important to note that these estimators cannot be obtained in explicit analytical forms. Instead, the estimation process involves solving a system of two non-linear equations in order to compute the MLEs. The non-linear nature of the equations makes it necessary to employ numerical methods or optimization algorithms to find the solutions. Iterative techniques such as Newton–Raphson or gradient-based algorithms are commonly used to solve the system of equations and obtain the MLEs. These methods iteratively update the parameter estimates until convergence is achieved, ensuring that the likelihood function is maximized. The two non-linear equations are given by

$$
\begin{aligned}
\frac{\partial}{\partial\alpha}\lambda(\alpha,\sigma) = {} & \frac{n}{\alpha} - \sigma\sum_{i=1}^{n}(\log w_i)w_i^{\alpha} - \frac{\sigma\pi}{2}\sum_{i=1}^{n}(\log w_i)w_i^{\alpha}e^{-\sigma w_i^{\alpha}}\csc^2\left[\frac{\pi}{2}e^{-\sigma w_i^{\alpha}}\right] \\
& + \frac{\sigma\pi}{2}\sum_{i=1}^{n}\frac{(\log w_i)w_i^{\alpha}e^{-\sigma w_i^{\alpha}}\csc^2\left(\frac{\pi}{2}e^{-\sigma w_i^{\alpha}}\right)\left[\pi e^{-\sigma w_i^{\alpha}}\cot\left(\frac{\pi}{2}e^{-\sigma w_i^{\alpha}}\right)-1\right]}{\left[1+\frac{\pi}{2}e^{-\sigma w_i^{\alpha}}\csc^2\left(\frac{\pi}{2}e^{-\sigma w_i^{\alpha}}\right)\right]} \\
& + \sum_{i=1}^{n}\log w_i,
\end{aligned}
$$

and

$$
\begin{aligned}
\frac{\partial}{\partial\sigma}\lambda(\alpha,\sigma) = {} & \frac{n}{\sigma} - \sum_{i=1}^{n}w_i^{\alpha} - \frac{\pi}{2}\sum_{i=1}^{n}w_i^{\alpha}e^{-\sigma w_i^{\alpha}}\csc^2\left[\frac{\pi}{2}e^{-\sigma w_i^{\alpha}}\right] \\
& + \frac{\pi}{2}\sum_{i=1}^{n}\frac{w_i^{\alpha}e^{-\sigma w_i^{\alpha}}\csc^2\left(\frac{\pi}{2}e^{-\sigma w_i^{\alpha}}\right)\left[\pi e^{-\sigma w_i^{\alpha}}\cot\left(\frac{\pi}{2}e^{-\sigma w_i^{\alpha}}\right)-1\right]}{\left[1+\frac{\pi}{2}e^{-\sigma w_i^{\alpha}}\csc^2\left(\frac{\pi}{2}e^{-\sigma w_i^{\alpha}}\right)\right]},
\end{aligned}
$$

Upon equating and solving $\frac{\partial}{\partial\alpha}\lambda(\alpha,\sigma)$ and $\frac{\partial}{\partial\sigma}\lambda(\alpha,\sigma)$ to zero, we obtain, respectively, the MLEs $\hat{\alpha}_{MLE}$ and $\hat{\sigma}_{MLE}$.

The asymptotic variance–covariance matrix is a crucial component in statistical inference, as it provides valuable information about the precision and uncertainty of the maximum likelihood estimators (MLEs). In order to obtain this matrix, an important step involves inverting the information matrix. The elements of the information matrix are derived from the expected values of the second-order derivatives of the logarithms of the likelihood functions. By taking the negative expected values of these second-order derivatives, the information matrix is constructed. Inverting this matrix yields the asymptotic variance–covariance matrix, which represents the approximate covariance structure of the MLEs.

In the present situation, it seems appropriate to approximate the expected values by their maximum likelihood estimates [25]. Accordingly, we have as the approximate variance–covariance matrix

$$
\begin{bmatrix} -I_{11} & -I_{12} \\ -I_{21} & -I_{22} \end{bmatrix}^{-1} = \begin{bmatrix} V(\hat{\alpha}) & Cov(\hat{\alpha},\hat{\sigma}) \\ Cov(\hat{\alpha},\hat{\sigma}) & V(\hat{\sigma}) \end{bmatrix},
$$

where

$$
\begin{aligned}
I_{11} = {} & \frac{\partial^2\lambda(\alpha,\sigma)}{\partial\alpha^2}|_{\hat{\alpha},\hat{\sigma}} = -\frac{n}{\alpha^2} + \sum_{i=1}^{n}\left[\frac{1}{2}\pi\sigma^2 w_i^{2\alpha}\log^2(w_i)e^{-\sigma w_i^{\alpha}}\csc^2\left(\frac{1}{2}\pi e^{-\sigma w_i^{\alpha}}\right)\right. \\
& - \frac{1}{2}\pi^2\sigma^2 w_i^{2\alpha}\log^2(w_i)e^{-2\sigma w_i^{\alpha}}\cot\left(\frac{1}{2}\pi e^{-\sigma w_i^{\alpha}}\right)\csc^2\left(\frac{1}{2}\pi e^{-\sigma w_i^{\alpha}}\right) - 2\sigma w_i^{\alpha}\log^2(w_i) \\
& \left. - \frac{1}{2}\pi\sigma w_i^{\alpha}\log^2(w_i)e^{-\sigma w_i^{\alpha}}\csc^2\left(\frac{1}{2}\pi e^{-\sigma w_i^{\alpha}}\right)\right] + \sum_{i=1}^{n}\left[\left(2\sigma w_i^{\alpha}\log(w_i)e^{\sigma w_i^{\alpha}}\right.\right. \\
& \left. + \pi^2\sigma w_i^{\alpha}\log(w_i)e^{-\sigma w_i^{\alpha}}\cot\left(\frac{1}{2}\pi e^{-\sigma w_i^{\alpha}}\right)\csc^2\left(\frac{1}{2}\pi e^{-\sigma w_i^{\alpha}}\right)\right)\left(-\frac{2\sigma w_i^{\alpha}\log(w_i)e^{\sigma w_i^{\alpha}}}{\left(2e^{\sigma w_i^{\alpha}}+\pi\csc^2\left(\frac{1}{2}\pi e^{-\sigma w_i^{\alpha}}\right)\right)^2}\right. \\
& \left. - \frac{\pi^2\sigma w_i^{\alpha}\log(w_i)e^{-\sigma w_i^{\alpha}}\cot\left(\frac{1}{2}\pi e^{-\sigma w_i^{\alpha}}\right)\csc^2\left(\frac{1}{2}\pi e^{-\sigma w_i^{\alpha}}\right)}{\left(2e^{\sigma w_i^{\alpha}}+\pi\csc^2\left(\frac{1}{2}\pi e^{-\sigma w_i^{\alpha}}\right)\right)^2}\right) + \frac{1}{2e^{\sigma w_i^{\alpha}}+\pi\csc^2\left(\frac{1}{2}\pi e^{-\sigma w_i^{\alpha}}\right)} \\
& \left(2\sigma w_i^{\alpha}\log^2(w_i)e^{\sigma w_i^{\alpha}} + \pi^2\sigma w_i^{\alpha}\log^2(w_i)e^{-\sigma w_i^{\alpha}}\cot\left(\frac{1}{2}\pi e^{-\sigma w_i^{\alpha}}\right)\csc^2\left(\frac{1}{2}\pi e^{-\sigma w_i^{\alpha}}\right)\right. \\
& + 2\sigma^2 w_i^{2\alpha}\log^2(w_i)e^{\sigma w_i^{\alpha}} - \pi^2\sigma^2 w_i^{2\alpha}\log^2(w_i)e^{-\sigma w_i^{\alpha}}\cot\left(\frac{1}{2}\pi e^{-\sigma w_i^{\alpha}}\right)\csc^2\left(\frac{1}{2}\pi e^{-\sigma w_i^{\alpha}}\right) \\
& \frac{1}{2}\pi^3\sigma^2 w_i^{2\alpha}\log^2(w_i)e^{-2\sigma w_i^{\alpha}}\csc^4\left(\frac{1}{2}\pi e^{-\sigma w_i^{\alpha}}\right) + \pi^3\sigma^2 w_i^{2\alpha}\log^2(w_i) \\
& \left.\left. + e^{-2\sigma w_i^{\alpha}}\cot^2\left(\frac{1}{2}\pi e^{-\sigma w_i^{\alpha}}\right)\csc^2\left(\frac{1}{2}\pi e^{-\sigma w_i^{\alpha}}\right)\right)\right],
\end{aligned}
$$

$$
\begin{aligned}
I_{12} = I_{21} = \frac{\partial^2 \lambda(\alpha,\sigma)}{\partial\alpha\partial\sigma}|_{\hat{\alpha},\hat{\sigma}} = \sum_{i=1}^{n} \Bigg(& - \frac{1}{2}\pi w_i^{\alpha} \log(w_i) e^{-\sigma w_i^{\alpha}} \csc^2\left(\frac{1}{2}\pi e^{-\sigma w_i^{\alpha}}\right) \\
& - \frac{1}{2}\pi^2 \sigma w_i^{2\alpha} \log(w_i) e^{-2\sigma w_i^{\alpha}} \cot\left(\frac{1}{2}\pi e^{-\sigma w_i^{\alpha}}\right) \csc^2\left(\frac{1}{2}\pi e^{-\sigma w_i^{\alpha}}\right) - 2w_i^{\alpha}\log(w_i) \\
& + \frac{1}{2}\pi\sigma w_i^{2\alpha} \log(w_i) e^{-\sigma w_i^{\alpha}} \csc^2\left(\frac{1}{2}\pi e^{-\sigma w_i^{\alpha}}\right)\Bigg) + \sum_{i=1}^{n}\Bigg[\Bigg(- \frac{2w_i^{\alpha} e^{\sigma w_i^{\alpha}}}{\left(2e^{\sigma w_i^{\alpha}} + \pi\csc^2\left(\frac{1}{2}\pi e^{-\sigma w_i^{\alpha}}\right)\right)^2} \\
& - \frac{\pi^2 w_i^{\alpha} e^{-\sigma w_i^{\alpha}} \cot\left(\frac{1}{2}\pi e^{-\sigma w_i^{\alpha}}\right)\csc^2\left(\frac{1}{2}\pi e^{-\sigma w_i^{\alpha}}\right)}{\left(2e^{\sigma w_i^{\alpha}} + \pi\csc^2\left(\frac{1}{2}\pi e^{-\sigma w_i^{\alpha}}\right)\right)^2}\Bigg)\Bigg(2\sigma w_i^{\alpha}\log(w_i) e^{\sigma w_i^{\alpha}} \\
& + \pi^2 \sigma w_i^{\alpha} \log(w_i) e^{-\sigma w_i^{\alpha}} \cot\left(\frac{1}{2}\pi e^{-\sigma w_i^{\alpha}}\right)\csc^2\left(\frac{1}{2}\pi e^{-\sigma w_i^{\alpha}}\right)\Bigg) + \frac{1}{2e^{\sigma w_i^{\alpha}} + \pi\csc^2\left(\frac{1}{2}\pi e^{-\sigma w_i^{\alpha}}\right)} \\
& \Bigg(2w_i^{\alpha}\log(w_i)e^{\sigma w_i^{\alpha}} + \pi^2 w_i^{\alpha}\log(w_i) e^{-\sigma w_i^{\alpha}}\cot\left(\frac{1}{2}\pi e^{-\sigma w_i^{\alpha}}\right)\csc^2\left(\frac{1}{2}\pi e^{-\sigma w_i^{\alpha}}\right) \\
& + 2\sigma w_i^{2\alpha}\log(w_i)e^{\sigma w_i^{\alpha}} - \pi^2\sigma w_i^{2\alpha}\log(w_i)e^{-\sigma w_i^{\alpha}}\cot\left(\frac{1}{2}\pi e^{-\sigma w_i^{\alpha}}\right)\csc^2\left(\frac{1}{2}\pi e^{-\sigma w_i^{\alpha}}\right) \\
& \frac{1}{2}\pi^3\sigma w_i^{2\alpha}\log(w_i)e^{-2\sigma w_i^{\alpha}}\csc^4\left(\frac{1}{2}\pi e^{-\sigma w_i^{\alpha}}\right) + \pi^3\sigma w_i^{2\alpha}\log(w_i) \\
& + e^{-2\sigma w_i^{\alpha}}\cot^2\left(\frac{1}{2}\pi e^{-\sigma w_i^{\alpha}}\right)\csc^2\left(\frac{1}{2}\pi e^{-\sigma w_i^{\alpha}}\right)\Bigg)\Bigg]
\end{aligned}
$$

$$
\begin{aligned}
I_{22} = \frac{\partial^2\lambda(\alpha,\sigma)}{\partial\sigma^2}|_{\hat{\alpha},\hat{\sigma}} = & -\frac{n}{\sigma^2} + \sum_{i=1}^{n}\left(\frac{1}{2}\pi w_i^{2\alpha}e^{-\sigma w_i^{\alpha}}\csc^2\left(\frac{1}{2}\pi e^{-\sigma w_i^{\alpha}}\right) - \frac{1}{2}\pi^2 w_i^{2\alpha}e^{-2\sigma w_i^{\alpha}}\cot\left(\frac{1}{2}\pi e^{-\sigma w_i^{\alpha}}\right)\right. \\
& \left.\csc^2\left(\frac{1}{2}\pi e^{-\sigma w_i^{\alpha}}\right)\right) + \sum_{i=1}^{n}\Bigg[\left(2w_i^{\alpha}e^{\sigma w_i^{\alpha}} + \pi^2 w_i^{\alpha}e^{-\sigma w_i^{\alpha}}\cot\left(\frac{1}{2}\pi e^{-\sigma w_i^{\alpha}}\right)\csc^2\left(\frac{1}{2}\pi e^{-\sigma w_i^{\alpha}}\right)\right) \\
& \left(-\frac{2w_i^{\alpha}e^{\sigma w_i^{\alpha}}}{\left(2e^{\sigma w_i^{\alpha}} + \pi\csc^2\left(\frac{1}{2}\pi e^{-\sigma w_i^{\alpha}}\right)\right)^2} - \frac{\pi^2 w_i^{\alpha}e^{-\sigma w_i^{\alpha}}\cot\left(\frac{1}{2}\pi e^{-\sigma w_i^{\alpha}}\right)\csc^2\left(\frac{1}{2}\pi e^{-\sigma w_i^{\alpha}}\right)}{\left(2e^{\sigma w_i^{\alpha}} + \pi\csc^2\left(\frac{1}{2}\pi e^{-\sigma w_i^{\alpha}}\right)\right)^2}\right) \\
& + \left(2e^{\sigma w_i^{\alpha}} + \pi\csc^2\left(\frac{1}{2}\pi e^{-\sigma w_i^{\alpha}}\right)\right)^{-1}\left(2w_i^{2\alpha}e^{\sigma w_i^{\alpha}} - \pi^2 w_i^{2\alpha}e^{-\sigma w_i^{\alpha}}\cot\left(\frac{1}{2}\pi e^{-\sigma w_i^{\alpha}}\right)\csc^2\left(\frac{1}{2}\pi e^{-\sigma w_i^{\alpha}}\right)\right) \\
& s\left(\frac{1}{2}\pi^3 w_i^{2\alpha}e^{-2\sigma w_i^{\alpha}}\csc^4\left(\frac{1}{2}\pi e^{-\sigma w_i^{\alpha}}\right) + \pi^3 w_i^{2\alpha} + e^{-2\sigma w_i^{\alpha}}\cot^2\left(\frac{1}{2}\pi e^{-\sigma w_i^{\alpha}}\right)\csc^2\left(\frac{1}{2}\pi e^{-\sigma w_i^{\alpha}}\right)\right)\Bigg]
\end{aligned}
$$

4.2. Simulation

This subsection describes the performances of $\hat{\alpha}_{MLE}$ and $\hat{\sigma}_{MLE}$ through Monte Carlo SS. The SS of the NCT-Weibull distribution is carried out for three different combination values of α and σ. These combination values are

- $\alpha = 0.9$ and $\sigma = 1.5$;
- $\alpha = 1.6$ and $\sigma = 1.2$;
- $\alpha = 1.5$ and $\sigma = 1$.

For all these three combination values, random numbers are generated from the NCT-Weibull distribution using the QF (it is also referred to as inverse CDF) with the help of an R-script. For each combination value, the random numbers $n = 50, 100, 200, 300, \ldots 5000$ are generated.

After obtaining the random numbers, the next step is calculating the evaluating criteria for judging the performances of $\hat{\alpha}_{MLE}$ and $\hat{\sigma}_{MLE}$. For this purpose, we choose two evaluating criteria, including

- Bias

$$\frac{1}{1000}\sum_{i=1}^{1000}\left(\hat{\xi}_i-\xi\right).$$

- Mean square error (MSE)

$$\frac{1}{1000}\sum_{i=1}^{1000}\left(\hat{\xi}_i-\xi\right)^2.$$

The numerical values of the MLEs and their evaluating criteria are computed using `optim()` with the help of R software. The results of the Monte Carlo SS of the NCT-Weibull distribution are presented in Tables 2–4.

From Tables 2–4, we reach the conclusion that as the value of n increases, the values of the

- MLEs $\hat{\alpha}_{MLE}$ and $\hat{\sigma}_{MLE}$ get closer and closer to the true value;
- MSEs of $\hat{\alpha}_{MLE}$ and $\hat{\sigma}_{MLE}$ decrease;
- Biases of $\hat{\alpha}_{MLE}$ and $\hat{\sigma}_{MLE}$ go to zero.

Table 2. The numerical description of the SS of the NCT-Weibull distribution for $\alpha = 0.9$ and $\sigma = 1.5$.

n	Parameters	MLE	MSE	Bias
	α	0.9355044	0.01082877	0.035504420
50	σ	1.5807460	0.06715720	0.080745775
	α	0.9201044	0.00479964	0.020104365
100	σ	1.5444920	0.03049332	0.044492288
	α	0.9151175	0.00277550	0.015117474
200	σ	1.5243870	0.01430133	0.024387130
	α	0.9105759	0.00186720	0.010575924
300	σ	1.5193200	0.00989402	0.019319599
	α	0.9084876	0.00125306	0.008487576
400	σ	1.5145360	0.00661767	0.014535798
	α	0.9073618	0.00094190	0.007361801
500	σ	1.5099910	0.00507208	0.009991227
	α	0.9048286	0.00076818	0.004828569
1000	σ	1.5098150	0.00412407	0.009415482
	α	0.9046138	0.00062513	0.004613809
1500	σ	1.5079170	0.00356039	0.008917051
	α	0.9045965	0.00058086	0.004596521
2000	σ	1.504196	0.00286160	0.004196165
	α	0.9040372	0.00043847	0.004507215
2500	σ	1.5038410	0.00201378	0.003840787
	α	0.9030904	0.00037242	0.004190369
3000	σ	1.5027150	0.00215174	0.003315493
	α	0.9022970	0.00035733	0.004096963
3500	σ	1.5018020	0.00162623	0.002802116
	α	0.9014026	0.00022969	0.003402595
4000	σ	1.5011270	0.00132665	0.002427410
	α	0.9010336	0.00022699	0.002733606
4500	σ	1.5003060	0.00110904	0.002005540
	α	0.9002476	0.00020651	0.001147633
5000	σ	1.5001260	0.00108060	0.004276054

MLE = maximum likelihood estimator, MSE = mean square error, n = sample size.

Table 3. The numerical description of the SS of the NCT-Weibull distribution for $\alpha = 1.6$ and $\sigma = 1.2$.

n	Parameters	MLE	MSE	Bias
	α	1.647293	0.03745800	0.04729255
50	σ	1.257434	0.04245403	0.05743403
	α	1.627257	0.01732586	0.02725739
100	σ	1.235155	0.01727730	0.03515506
	α	1.618928	0.00993020	0.01892835
200	σ	1.216921	0.00978696	0.01692071
	α	1.610806	0.00749452	0.01080646
300	σ	1.209155	0.00590437	0.00915519
	α	1.607756	0.00578927	0.00875570
400	σ	1.207724	0.00522039	0.00772403
	α	1.607377	0.00495649	0.00837722
500	σ	1.206386	0.00413462	0.00638614
	α	1.607077	0.00404159	0.00807700
1000	σ	1.204783	0.00370541	0.00608253
	α	1.605926	0.00357296	0.00592560
1500	σ	1.202933	0.00310211	0.00553341
	α	1.605566	0.00342711	0.00506591
2000	σ	1.201824	0.00299849	0.00524317
	α	1.603931	0.00269719	0.00430580
2500	σ	1.201376	0.00258171	0.00437642
	α	1.603272	0.00248891	0.00427248
3000	σ	1.201039	0.00238806	0.00383875
	α	1.602213	0.00226258	0.00381321
3500	σ	1.200925	0.00215743	0.00332455
	α	1.601890	0.00211945	0.00338986
4000	σ	1.200769	0.00206960	0.00286931
	α	1.600817	0.00197970	0.00301707
4500	σ	1.200167	0.00170270	0.00216691
	α	1.600798	0.00118820	0.00149835
5000	σ	1.200115	0.00124240	0.00139478

MLE = maximum likelihood estimator, MSE = mean square error, *n* = sample size.

Table 4. The numerical description of the SS of the NCT-Weibull distribution for $\alpha = 1.5$ and $\sigma = 1$.

n	Parameters	MLE	MSE	Bias
	α	1.536557	0.02935531	0.036556898
50	σ	1.032626	0.02028196	0.032626058
	α	1.523453	0.01454322	0.023453154
100	σ	1.022780	0.01560843	0.022780097
	α	1.512594	0.00878291	0.018594240
200	σ	1.012194	0.00617592	0.012193633
	α	1.512682	0.00751053	0.012682101
300	σ	1.011429	0.00479729	0.011428825
	α	1.509734	0.00474624	0.009734084
400	σ	1.008920	0.00435279	0.008920038
	α	1.506511	0.00435750	0.007510780
500	σ	1.008418	0.00389977	0.007417519

Table 4. *Cont.*

n	Parameters	MLE	MSE	Bias
1000	α	1.505726	0.00376879	0.006726321
	σ	1.007672	0.00348127	0.007071814
1500	α	1.505137	0.00321440	0.005837298
	σ	1.006518	0.00312391	0.005518071
2000	α	1.503928	0.00292193	0.005128123
	σ	1.005165	0.00296230	0.004164561
2500	α	1.502614	0.00273244	0.004613729
	σ	1.004497	0.00250790	0.003497397
3000	α	1.501920	0.00244730	0.003920174
	σ	1.003782	0.00201760	0.002781555
3500	α	1.501252	0.00220965	0.002252233
	σ	1.002927	0.00143502	0.002427178
4000	α	1.501022	0.00181327	0.001721648
	σ	1.002255	0.00130605	0.002254885
4500	α	1.500701	0.00144591	0.001300919
	σ	1.002055	0.00118396	0.002055212
5000	α	1.500362	0.00106532	0.000932209
	σ	1.004314	0.00113503	0.001313930

MLE = maximum likelihood estimator, MSE = mean square error, n = sample size.

5. Data Analyses

This section demonstrates and validates the applicability of the NCT-Weibull distribution by considering two practical examples (i.e., analyzing two datasets). Both examples are based on the use of medical datasets. We apply the NCT-Weibull distribution to both medical datasets in comparison with some rival distributions.

5.1. Description of the Datasets

This subsection provides a description of medical datasets that are considered to demonstrate and validate the applicability of the NCT-Weibull distribution.

The first dataset (this can be represented by Data 1) represents the survival times (measured in years) of the patients. This dataset consists of the survival times of 45 patients who received chemotherapy treatment; see [26,27]. The second dataset (represented by Data 2) also represents the survival times (measured in weeks) of the patients. Data 2 consists of survival times for 32 patients diagnosed with acute myelogenous leukemia [28].

Some key measures (i.e., summary measures) of Data 1 and Data 2 are presented in Table 5. Additionally, some key plots of Data 1 and Data 2 are also shown, respectively, in Figures 5 and 6.

Table 5. Key measures of the chemotherapy and acute myelogenous leukemia data.

Description	Mean	1st Quartile	2nd Quartile	3rd Quartile
Data 1	1.341	0.395	0.841	2.178
Data 2	42.060	4.000	22.000	65.000
Description	Standard deviation	Variance	Minimum	Maximum
Data 1	1.246	1.554	0.047	4.033
Data 2	46.944	2203.802	1.00	156.00
Description	Range	Skewness	Kurtosis	Data size
Data 1	3.986	0.972	2.663	45
Data 2	155	1.124	3.026	32

Data 1 = Chemotherapy dataset, Data 2 = Myelogenous leukemia dataset.

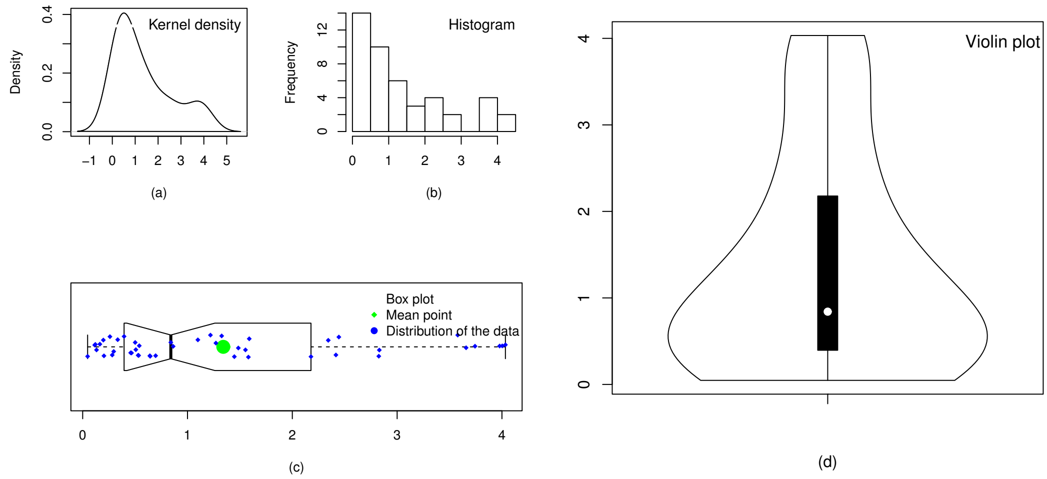

Figure 5. The chemotherapy dataset represented by (**a**) kernel density plot, (**b**) histogram, (**c**) box plot, and (**d**) violin plot.

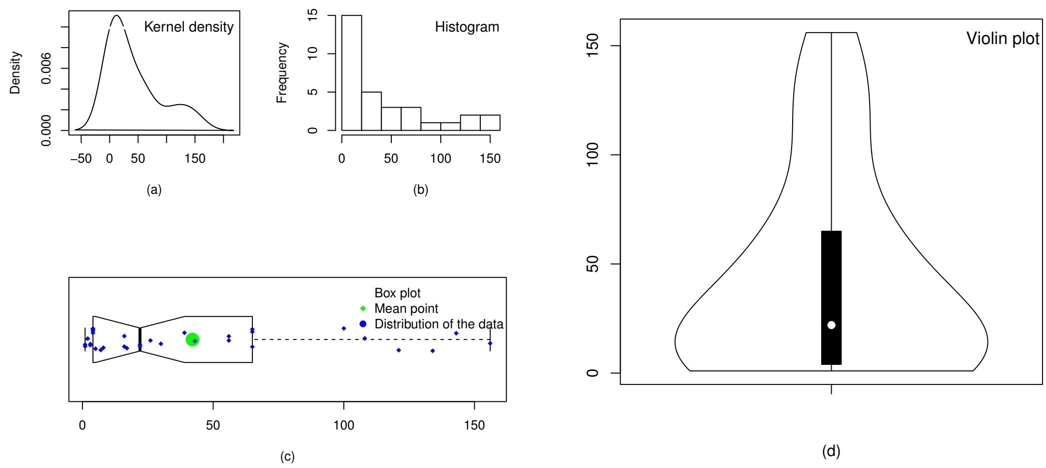

Figure 6. The acute myelogenous leukemia dataset represented by (**a**) kernel density plot, (**b**) histogram, (**c**) box plot, and (**d**) violin plot.

5.2. The Rival Distributions and Decisive Measures

This subsection presents some rival distributions that are considered alternative models for analyzing Data 1 and Data 2. The rival distributions include the (i) Weibull distribution (two-parameter model), (ii) new extended exponential Weibull (NEE-Weibull) distribution, which is a three-parameter model, and (iii) new alpha cosine Weibull (NAC-Weibull) distribution, which is also a three-parameter model.

The proposed NCT-Weibull distribution is applied to medical datasets (which are described above) with these rival distributions to determine its utility and best fit compared to the rival distributions. The distribution functions of the rival distribution are given by

- Weibull distribution

$$G(w;\boldsymbol{\xi}) = 1 - e^{-\sigma w^{\alpha}}, \qquad w \geq 0, \alpha > 0, \sigma > 0.$$

- NEE-Weibull distribution

$$G(w;\beta,\boldsymbol{\xi}) = 1 - \frac{\beta e^{-\sigma w^{\alpha}}}{\beta + 1 - e^{-\sigma w^{\alpha}}}, \qquad w \geq 0, \alpha > 0, \sigma > 0, \beta > 0.$$

- NAC-Weibulll distribution

$$G(w;\alpha_1,\boldsymbol{\xi}) = \frac{\alpha_1^{\cos\left(\frac{\pi}{2}e^{-\sigma w^{\alpha}}\right)} - 1}{\alpha_1 - 1}, \qquad w \geq 0, \alpha > 0, \sigma > 0, \alpha_1 > 0, \alpha_1 \neq 1.$$

Now, we describe some decision tools that we apply to establish the superior performance (i.e., best fitting power) of the NCT-Weibull distribution over competing distributions using medical datasets. The decision-making tools consist of four information criteria (IC), calculated as follows:

- Akaike information criterion (AIC)

$$2k - 2\delta(.).$$

- Consistent Akaike information criterion (CAIC)

$$\frac{2nk}{n-k-1} - 2\delta(.).$$

- Bayesian information criterion (BIC)

$$k\log(n) - \delta(.).$$

- Hannan–Quinn information criterion (HQIC)

$$2k\log[\log(n)] - 2\delta(.).$$

In the expressions of decision-making tools, the quantities n, k, and $\delta(.)$ represent the size of the data, the number of model parameters, and the LLF of the fitted distribution, respectively.

Among the NCT-Weibull and rival distributions, the model with the lowest values of the decision-making tools is considered the best-suited model for the chemotherapy and acute myelogenous leukemia datasets.

5.3. Analysis of Data 1

The first example (i.e., the first illustration) of the NCT-Weibull distribution using survival times for chemotherapy patients is provided in this subsection. Corresponding to this dataset, the values of the MLEs $\hat{\alpha}, \hat{\sigma}, \hat{\beta}$ and $\hat{\alpha}_1$ of the NCT-Weibull distribution and rival models are reported in Table 6.

Furthermore, using the survival times of the chemotherapy patients' data, the uniqueness and existence of $\hat{\alpha}$ and $\hat{\sigma}$ of the NCT-Weibull distribution are shown visually in Figure 7 and Figure 8, respectively. The plots in Figure 7 show that $\hat{\alpha}$ and $\hat{\sigma}$ have unique solutions, whereas the plots in Figure 8 indicate the existence of the LLF, as each curve intersects the x-axis at one point.

Using the survival times of the chemotherapy patients' data, the values of the decisive measures of the NCT-Weibull and rival distributions are obtained in Table 6. Based on the reported results of the IC in Table 7, we can easily observe that the NCT-Weibull distribution has the smallest values, leading to the fact that the NCT-Weibull distribution is the most appropriate model for analyzing Data 1 as compared to rival distributions. For the NCT-Weibull distribution, the values of the IC quantities are AIC = 118.8058, CAIC = 119.0916, BIC = 122.4192, and HQIC = 120.1529. For this dataset, the second most appropriate model is the NEE-Weibull distribution with AIC = 121.6609, CAIC = 122.2462, BIC = 127.0808, and HQIC = 123.6814. The Weibull distribution ranked as the third most suitable model for analyzing the chemotherapy patients' dataset.

Having numerically demonstrated the appropriateness of the NCT-Weibull distribution for chemotherapy patient data, we now establish visually the appropriateness of the

NCT-Weibull distribution. For a visual illustration of the performance of the fitted distributions, we obtain the fitted plots of the NCT-Weibull and rival distributions. The fitted plots considered in this paper include empirical CDF, estimated PDF, and Kaplan–Meier survival plots; see Figures 9 and 10. Based on the plots in Figures 9 and 10, we can see that the NCT-Weibull distribution closely follows the chemotherapy patients' dataset.

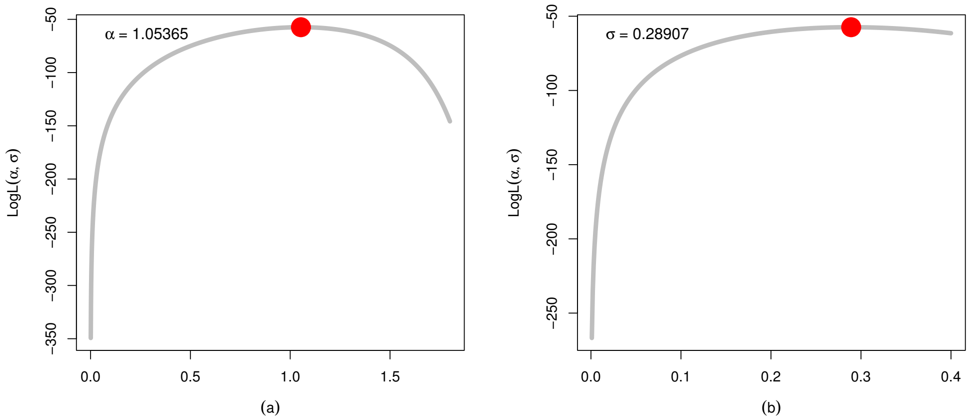

Figure 7. The profiles of the LLF of (**a**) $\hat{\alpha}_{MLE}$ and (**b**) $\hat{\sigma}_{MLE}$ of the NCT-Weibull distribution for the chemotherapy treatment dataset.

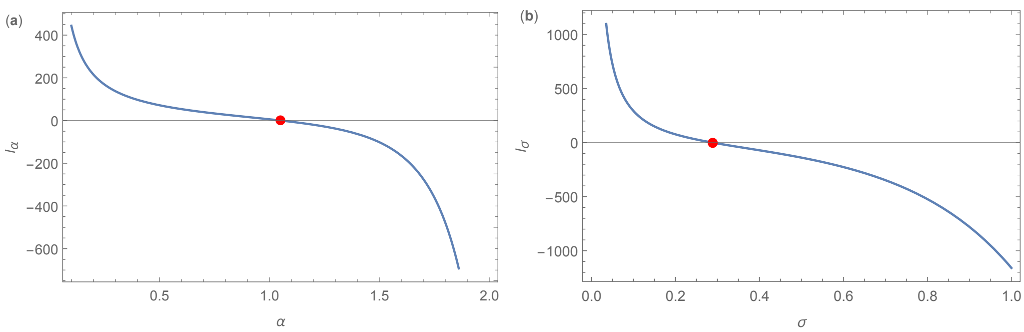

Figure 8. The visual illustrations of the existence of (**a**) $\hat{\alpha}_{MLE}$ and (**b**) $\hat{\sigma}_{MLE}$ of the NCT-Weibull distribution for the chemotherapy treatment dataset.

Table 6. The numerical values of $\hat{\alpha}, \hat{\sigma}, \hat{\beta}$, and $\hat{\alpha}_1$ of the fitted models for the chemotherapy treatment dataset.

Dist.	$\hat{\alpha}$	$\hat{\sigma}$	$\hat{\beta}$	$\hat{\alpha}_1$
NCT-Weibull	1.05365	0.28907	-	-
Weibull	1.05460	0.71613	-	-
NEE-Weibull	1.26571	0.38501	0.62759	-
NAC-Weibull	1.08096	0.33115	-	0.49814

Table 7. The values of the decisive tools of the NCT-Weibull and its rival probability distributions for the chemotherapy treatment dataset.

Dist.	**AIC**	**CAIC**	**BIC**	**HQIC**
NCT-Weibull	118.8058	119.0916	122.4192	120.1529
Weibull	122.2476	122.5334	125.8610	123.5947
NEE-Weibull	121.6609	122.2462	127.0808	123.6814
NAC-Weibull	122.2846	122.8700	127.7046	124.3052

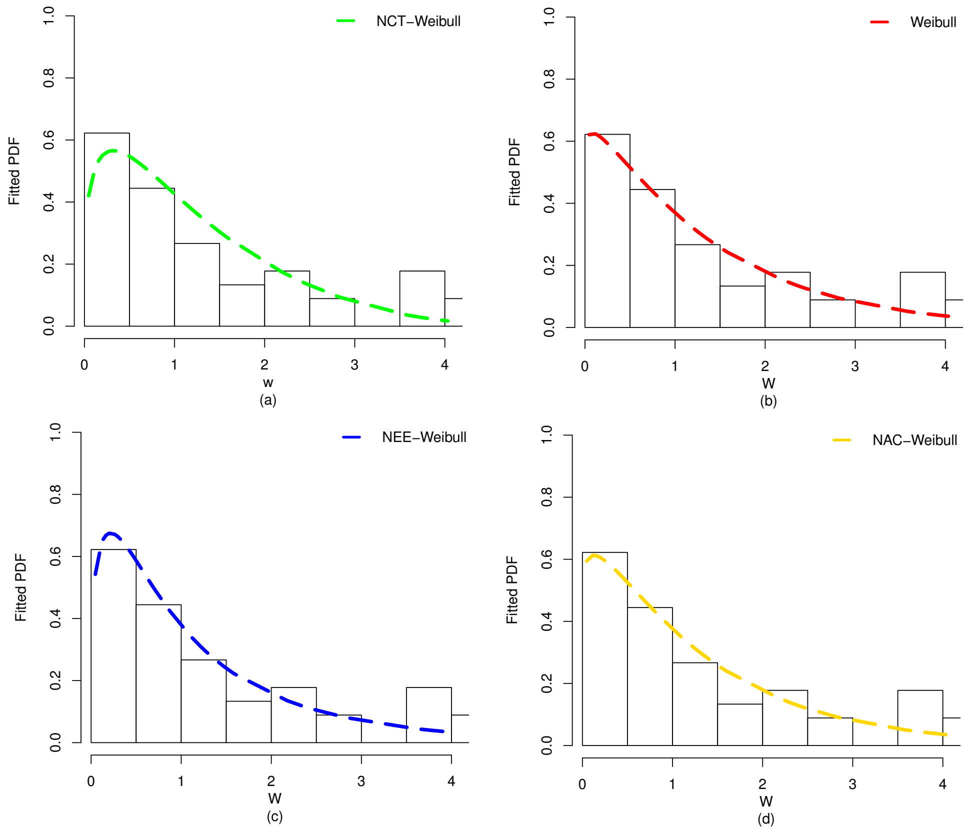

Figure 9. The fitted PDF plots of the (**a**) NCT-Weibull, (**b**) Weibull, (**c**) NEE-Weibull, and (**d**) NAC-Weibull for the chemotherapy treatment dataset.

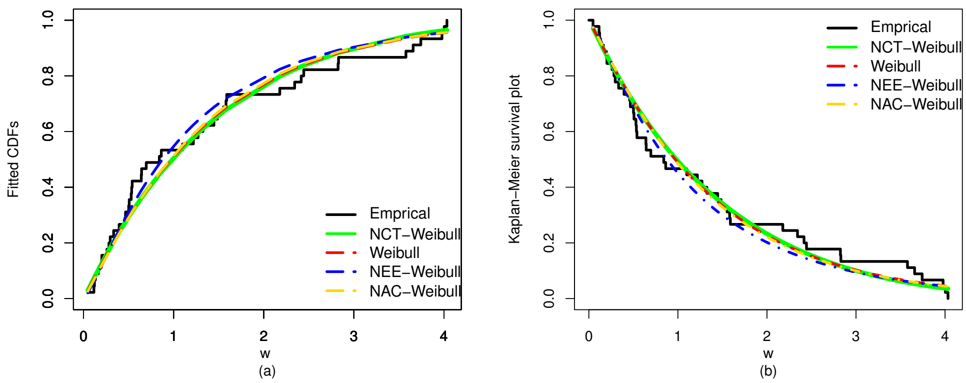

Figure 10. Corresponding to the chemotherapy treatment dataset, the fitted (**a**) CDF and (**b**) SF of the NCT-Weibull distribution and rival models.

5.4. Analysis of Data 2

This subsection presents another practical example of the NCT-Weibull distribution using the acute myelogenous leukemia dataset. The values of the MLEs $\hat{\alpha}, \hat{\sigma}, \hat{\beta}$, and $\hat{\alpha}_1$ of the NCT-Weibull and rival distribution are shown in Table 8.

Using the acute myelogenous leukemia dataset, we again show the uniqueness and existence of $\hat{\alpha}$ and $\hat{\sigma}$ of the NCT-Weibull distribution; see Figures 11 and 12. The plots in Figures 11 and 12 confirm the unique solutions and existence of $\hat{\alpha}$ and $\hat{\sigma}$ of the NCT-Weibull distribution, respectively.

Using the acute myelogenous leukemia dataset, the values of the decisive measures of the NCT-Weibull and rival distributions are reported in Table 9. Corresponding to the given results in Table 9, it is obvious that the NCT-Weibull distribution performs better than the Weibull, NEE-Weibull, and NAC-Weibull distributions. For the acute myelogenous leukemia dataset, the IC measures of the NCT-Weibull distribution are given by AIC = 303.0642, CAIC = 303.4780, BIC = 305.9956, and HQIC = 304.0359. For Data 2, the second most appropriate model is the Weibull distribution with AIC = 304.3037, CAIC = 304.7175, BIC = 307.2352, and HQIC = 305.2754. Similarly, the NEE-Weibull distribution and NAC-Weibull distribution are, respectively, ranked as the third and fourth most suitable models for analyzing the myelogenous leukemia dataset.

In addition to the numerical demonstration of the appropriateness of the NCT-Weibull distribution for the myelogenous leukemia dataset, we revisit the visual approach to demonstrate the suitability of the NCT-Weibull distribution. For the visual demonstration, we again consider the fitted plots that are discussed in the previous subsection; see Figures 13 and 14. The visual comparison, using the fitted plots in Figures 13 and 14, also confirms the appropriateness of the NCT-Weibull distribution for Data 2.

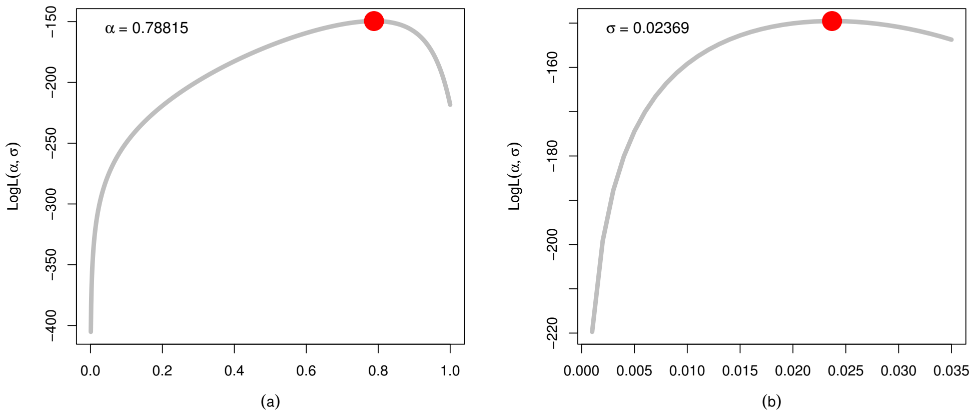

Figure 11. The profiles of the LLF of (**a**) $\hat{\alpha}_{MLE}$ and (**b**) $\hat{\sigma}_{MLE}$ of the NCT-Weibull distribution for the acute myelogenous leukemia dataset.

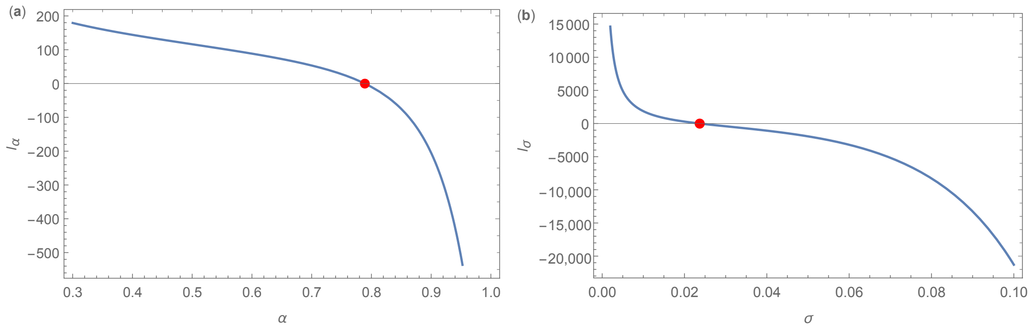

Figure 12. The visual illustrations of the existence of (**a**) $\hat{\alpha}_{MLE}$ and (**b**) $\hat{\sigma}_{MLE}$ of the NCT-Weibull distribution for the acute myelogenous leukemia dataset.

Table 8. The numerical values of $\hat{\alpha}, \hat{\sigma}, \hat{\beta}$, and $\hat{\alpha}_1$ of the fitted models for the acute myelogenous leukemia dataset.

Dist.	$\hat{\alpha}$	$\hat{\sigma}$	$\hat{\beta}$	$\hat{\alpha}_1$
NCT-Weibull	0.78815	0.02369	-	-
Weibull	0.79167	0.05780	-	-
NEE-Weibull	0.86363	0.03308	1.71726	-
NAC-Weibull	0.82236	0.02428	-	0.44785

Table 9. The values of the decisive tools of the NCT-Weibull and its rival probability distributions for the acute myelogenous leukemia dataset.

Dist.	AIC	CAIC	BIC	HQIC
NCT-Weibull	303.0642	303.4780	305.9956	304.0359
Weibull	304.3037	304.7175	307.2352	305.2754
NEE-Weibull	306.1248	306.9820	310.5221	307.5824
NAC-Weibull	306.5065	307.3637	310.9037	307.9641

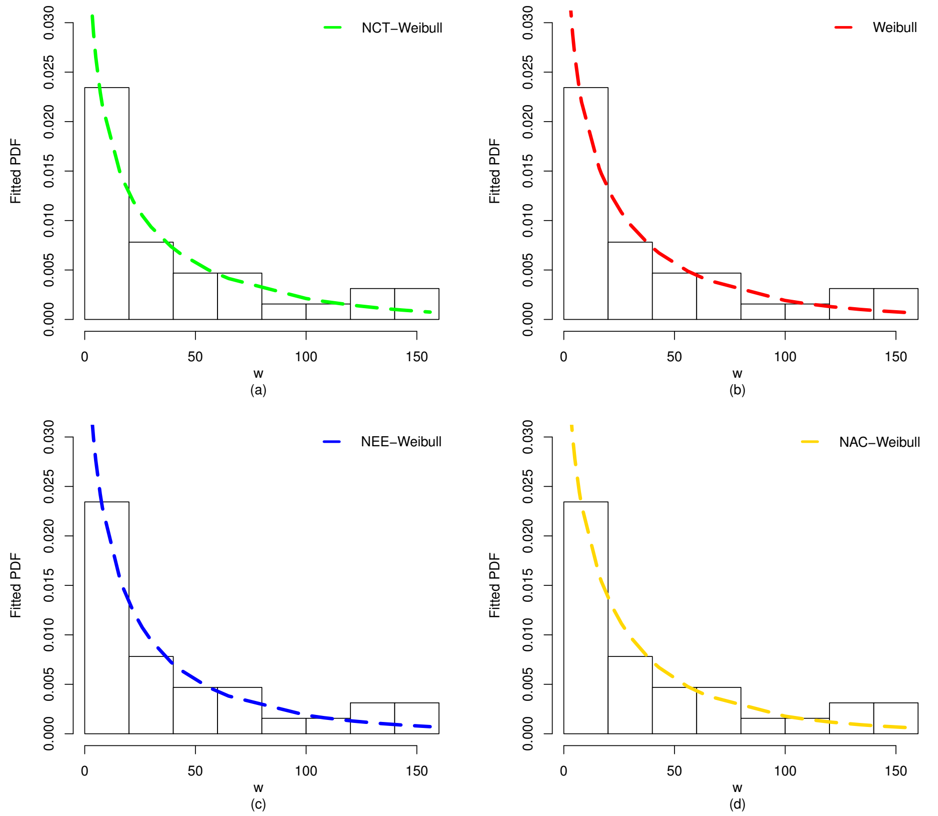

Figure 13. The fitted PDF plots of the (**a**) NCT-Weibull, (**b**) Weibull, (**c**) NEE-Weibull, and (**d**) NAC-Weibull for the acute myelogenous leukemia dataset.

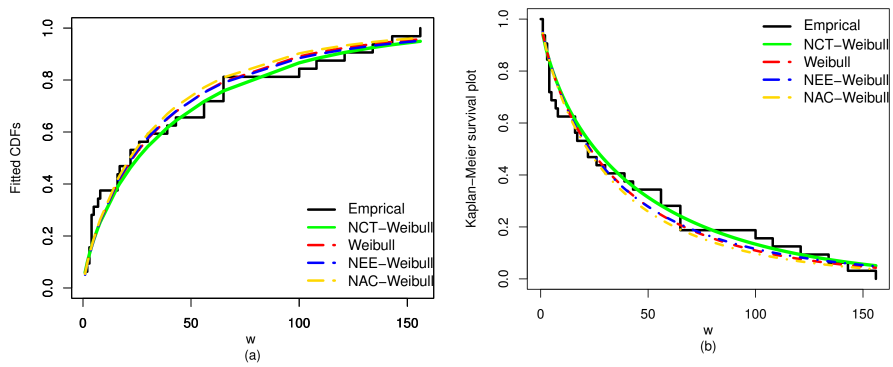

Figure 14. Corresponding to the acute myelogenous leukemia dataset, the fitted (**a**) CDF and (**b**) SF of the NCT-Weibull distribution and rival models.

6. Concluding Remarks

Probability distributions have wider applications in almost every field of life. However, no probability distribution provides a satisfactory fit to all types of datasets. Therefore, introducing new probability distributions with better fitting power is an important research topic, and the demand for it is increasing rapidly. Because of the practical importance of probability distributions, researchers are focusing on the development of new probability distributions to meet the need. In this regard, so far, several new probability distributions with updated features have been developed and implemented. Often, the new probability distributions provide a better fit than the baseline model or other traditional models. But, in most cases, the number of parameters has also increased from one to seven. Additional parameters sometimes lead to re-parameterization problems.

In order to avoid re-parameterization problems as well as to update the fitting power and distributional flexibility of the baseline model, this paper introduced a new probabilistic method. The proposed method was based on the trigonometric function implementation and was named a new cotangent-*G* (NCT-*G*) family of distributions. Certain distributional properties of the NCT-*G* distributions were derived. A special member of the NCT-*G* distributions (taking the Weibull as the baseline model) called the NCT-Weibull distribution was considered for illustrative purposes. MLEs of the NCT-Weibull distribution were obtained. The uniqueness of the MLEs of the NCT-Weibull distribution was visually demonstrated using two practical datasets. Furthermore, the MLEs of the NCT-Weibull distribution were also evaluated by Monte Carlo SS using two statistical criteria. Finally, the practical importance of the NCT-Weibull distribution was demonstrated by considering two examples from the medical field. Based on the four ICs, it was shown that the NCT-Weibull distribution outperforms the Weibull distribution and its two other variants.

Author Contributions: Conceptualization, O.H.O., H.M.A. and Z.A.; methodology, O.H.O., H.M.A. and Z.A.; software, O.H.O., Z.A., F.K. and A.A.-A.H.E.-B.; validation, O.H.O. and Z.A.; formal analysis, H.M.A., O.H.O., Z.A. and F.K.; investigation, O.H.O. and A.A.-A.H.E.-B.; data curation, Z.A. and F.K.; writing—original draft preparation, O.H.O., H.M.A., Z.A., F.K. and A.A.-A.H.E.-B.; writing—review and editing, O.H.O., H.M.A. and Z.A.; visualization, H.M.A., Z.A., F.K. and A.A.-A.H.E.-B. All authors have read and agreed to the published version of the manuscript.

Funding: This research project was funded by the Deanship of Scientific Research, Princess Nourah bint Abdulrahman University, through the Program of Research Project Funding After Publication, grant No (44-PRFA-P-88).

Data Availability Statement: The data sets are available from the corresponding author upon request.

Conflicts of Interest: The authors declare no competing interest.

References

1. Alshanbari, H.M.; Ahmad, Z.; Khan, F.; Khosa, S.K.; Ilyas, M.; El-Bagoury, A.A.A.H. Univariate and multivariate analyses of the asset returns using new statistical models and penalized regression techniques. *Aims Math.* **2023**, *8*, 19477–19503. [CrossRef]
2. Alshanbari, H.M.; Abd El-Bagoury, A.A.H.; Gemeay, A.M.; Hafez, E.H.; Eldeeb, A.S. A flexible extension of pareto distribution: Properties and applications. *Comput. Intell. Neurosci.* **2021**, *2021*, 9819200. [CrossRef]
3. Makubate, B.; Gabanakgosi, M.; Chipepa, F.; Oluyede, B. A new Lindley-Burr XII power series distribution: Model, properties and applications. *Heliyon* **2021**, *7*, e07146. [CrossRef]
4. Almuqrin, M.A.; Gemeay, A.M.; El-Raouf, M.A.; Kilai, M.; Aldallal, R.; Hussam, E. A flexible extension of reduced kies distribution: Properties, inference, and applications in biology. *Complexity* **2022**, *2022*, 6078567. [CrossRef]
5. Eghwerido, J.T.; Agu, F.I. The statistical properties and applications of the alpha power Topp-Leone-G distribution. *Heliyon* **2022**, *8*, e09775. [CrossRef] [PubMed]
6. Eghwerido, J.T.; Nzei, L.C.; Omotoye, A.E.; Agu, F.I. The Teissier-G family of distributions: Properties and applications. *Math. Slovaca* **2022**, *72*, 1301–1318. [CrossRef]
7. El-Morshedy, M.; Eliwa, M.S.; Tyagi, A. A discrete analogue of odd Weibull-G family of distributions: Properties, classical and Bayesian estimation with applications to count data. *J. Appl. Stat.* **2022**, *49*, 2928–2952. [CrossRef]
8. Atchadé, M.N.; N'bouké, M.; Djibril, A.M.; Shahzadi, S.; Hussam, E.; Aldallal, R.; Alshanbari, H.M.; Gemeay, A.M.; El-Bagoury, A.A.H. A New Power Topp–Leone distribution with applications to engineering and industry data. *PLoS ONE* **2023**, *18*, e0278225. [CrossRef] [PubMed]
9. Althubyani, F.A.; Abd El-Bar, A.M.; Fawzy, M.A.; Gemeay, A.M. A New 3-Parameter Bounded Beta Distribution: Properties, Estimation, and Applications. *Axioms* **2022**, *11*, 504. [CrossRef]
10. Klakattawi, H.; Alsulami, D.; Elaal, M.A.; Dey, S.; Baharith, L. A new generalized family of distributions based on combining Marshal-Olkin transformation with TX family. *PLoS ONE* **2022**, *17*, e0263673. [CrossRef]

11. Nawel, K.; Gemeay, A.M.; Zeghdoudi, H.; Karakaya, K.; Alshangiti, A.M.; Bakr, M.E.; Balogun, O.S.; Muse, A.H.; Hussam, E. Modeling Voltage Real Data Set by a New Version of Lindley Distribution. *IEEE Access* **2023**, *11*, 67220–67229.
12. Arshad, M.Z.; Iqbal, M.Z.; Were, F.; Aldallal, R.; Riad, F.H.; Bakr, M.E.; Tashkandy, A.; Hussam, E.; Gemeay, A.M. An Alternative Statistical Model to Analysis Pearl Millet (Bajra) Yield in Province Punjab and Pakistan. *Complexity* **2023**, *2023*, 8713812. [CrossRef]
13. Albassam, M.; Ahsan-ul-Haq, M.; Aslam, M. Weibull distribution under indeterminacy with applications. *AIMS Math.* **2023**, *8*, 10745–10757. [CrossRef]
14. Tashk, Y.Y.; Emam, W. On Predictive Modeling Using a New Three-Parameters Modification of Weibull Distribution and Application. *Appl. Sci.* **2023**, *13*, 3909.
15. AlQdah, K.S.; Alahmdi, R.; Alansari, A.; Almoghamisi, A.; Abualkhair, M.; Awais, M. Potential of wind energy in Medina, Saudi Arabia based on Weibull distribution parameters. *Wind. Eng.* **2021**, *45*, 1652–1661. [CrossRef]
16. Sánchez, L.; Leiva, V.; Saulo, H.; Marchant, C.; Sarabia, J.M. A new quantile regression model and its diagnostic analytics for a Weibull distributed response with applications. *Mathematics* **2021**, *9*, 2768. [CrossRef]
17. Sarhan, A.M.; Zaindin, M. Modified Weibull distribution. *APPS. Appl. Sci.* **2009**, *11*, 123–136.
18. Silva, G.O.; Ortega, E.M.; Cordeiro, G.M. The beta modified Weibull distribution. *Lifetime Data Anal.* **2010**, *16*, 409–430. [CrossRef]
19. Barreto-Souza, W.; de Morais, A.L.; Cordeiro, G.M. The Weibull-geometric distribution. *J. Stat. Comput. Simul.* **2011**, *81*, 645–657. [CrossRef]
20. Almalki, S.J.; Yuan, J. A new modified Weibull distribution. *Reliab. Eng. Syst. Saf.* **2013**, *111*, 164–170. [CrossRef]
21. Rehman, H.; Chandra, N.; Hosseini-Baharanchi, F.S.; Baghestani, A.R.; Pourhoseingholi, M.A. Cause-specific hazard regression estimation for modified Weibull distribution under a class of non-informative priors. *J. Appl. Stat.* **2022**, *49*, 1784–1801. [CrossRef] [PubMed]
22. Almalki, S.J.; Nadarajah, S. Modifications of the Weibull distribution: A review. *Reliab. Eng. Syst. Saf.* **2014**, *124*, 32–55. [CrossRef]
23. Wais, P. A review of Weibull functions in wind sector. *Renew. Sustain. Energy Rev.* **2017**, *70*, 1099–1107.
24. Nofal, Z.M.; Afify, A.Z.; Yousof, H.M.; Granzotto, D.C.; Louzada, F. Kumaraswamy transmuted exponentiated additive Weibull distribution. *Int. J. Stat. Probab.* **2016**, *5*, 78–99. [CrossRef]
25. Cohen, A.C. Maximum likelihood estimation in the Weibull distribution based on complete and on censored samples. *Technometrics* **1965**, *7*, 579–588.
26. Bekker, A.; Roux, J.J.J.; Mosteit, P.J. A generalization of the compound Rayleigh distribution: Using a Bayesian method on cancer survival times. *Commun. Stat.- Theory Methods* **2000**, *29*, 1419–1433. [CrossRef]
27. Nwezza, E.E.; Ugwuowo, F.I. An extended normal distribution for reliability data analysis. *J. Stat. Manag. Syst.* **2022**, *25*, 369–392. [CrossRef]
28. Jamal, F.; Nasir, M.A.; Tahir, M.H.; Montazeri, N.H. The odd Burr-III family of distributions. *J. Stat. Appl. Probab.* **2017**, *6*, 105–122.